THERMALLY AND FRICTIONALLY PRODUCED WIND SHEAR IN THE PLANETARY BOUNDARY LAYER AT LITTLE AMERICA, ANTARCTICA

BERNHARD LETTAU

Institute for Atmospheric Sciences, ESSA, Silver Spring, Md.

ABSTRACT

Pilot balloon wind profiles obtained by the first and second Byrd Antarctic Expeditions are analyzed to show that the mean observed wind shear between the surface and 1,000 m. can be resolved into a frictional component which produces a normal boundary layer wind spiral, and a thermal component resulting from the temperature gradient at the ice edge, which deforms the normal wind spiral. Values of surface stress, surface Rossby number, geostrophic drag coefficient, energy dissipation, and roughness length derived from the wind profiles are collectively sufficiently different from values obtained over land or water surfaces, to suggest that the ice surface produces its own characteristic wind distribution.

1. INTRODUCTION

Little America Station was first established by the Byrd Antarctic Expedition at 78°34' S., 163°56' W., near the seaward edge of the Ross Ice Shelf in January 1929, and continuous meteorological measurements were obtained through February 1930. The base was reoccupied in March 1934 by the Second Byrd Antarctic Expedition and finally dismantled in February 1935 after another full year. Included in the data were 983 pilot balloon wind profiles—414 in 1929–30, and 569 in 1934–35—from which wind speeds and directions for standard levels at roughly 200-m. intervals have been tabulated and published (Grimminger and Haines [2]). In April 1940, the West Base of the United States Antarctic Service Expedition was established as Little America III, 7 mi. north-northeast of the camp of the Byrd expeditions. This station was operated until January 1941, and produced an additional 233 wind profiles, which, however, have not been used here.

In this preliminary study the individual mean wind shears between the surface and the top of the boundary layer have been separated into thermally and frictionally produced components, which are classified by season and by surface wind direction. Representative mean wind profiles are analyzed for various surface parameters in a later section.

2. WIND DATA

Within the planetary boundary layer of a barotropic atmosphere the wind profile is a function of the surface stress, the Coriolis parameter, and the horizontal pressure gradient. The resulting hodograph has a spiral form with the surface wind directed to the left of the free air geostrophic wind in the Northern Hemisphere, and approaching it asymptotically at the top of the boundary layer. In the Southern Hemisphere the surface wind is to the right of the geostrophic wind.

In the following discussion a Cartesian coordinate system will be used whose components are directed parallel and normal to the surface wind. Components along and to the right of the surface wind will be defined as positive. In this system, applied in the Southern Hemisphere, the wind vector at the top of the planetary boundary layer ($H=1,000$ m.) will generally have a positive parallel and a negative normal component.

The condition of barotropy is rarely fulfilled in the boundary layer, particularly not at Little America where the seaward edge of the Ross Ice Shelf provides a strong horizontal temperature contrast throughout the year. The relatively warm water to the north and the colder ice to the south produce a thermal wind parallel to the ice edge, generally toward the east, which will distort the simple spiral hodographs. Under the given geographical conditions the spiral will be elongated for westerly winds and foreshortened for east winds.

In preparation for the analysis, the surface and 1,000-m. wind readings were extracted from the pilot balloon observations at Little America for both the 1929–30 and 1934–35 seasons, and were grouped by surface wind direction and by season. The directional resolution was to 16 points, while the seasonal distribution was limited to summer (November to February), and winter (May to August). The directional distribution is asymmetric with a preponderance of observations of southerly winds at the surface. The least frequent wind direction was north-northwest with two cases, both occurring in summer;

the maximum number in each season was 47, for east winds in summer, and south-southwest winds in winter. It should be remembered, however, that, northwesterly onshore winds were generally accompanied by low cloud or fog, and that consequently the asymmetry is accentuated, if not caused entirely, by the lack of a 1,000-m. value. It is also true that when drifting snow or low clouds precluded a reasonably complete sounding the balloon launching schedule was suspended temporarily.

For each sounding that extended above a nominal altitude of 1,000 m. (tabulated as an actual 990 m.) the components of the 1,000-m. wind parallel and normal to the surface wind were obtained. The component values were then averaged by class, and the total shear, i.e., the differences between components at 1,000 m. and the surface, were calculated. The averaged values are given in table 1 by surface wind direction and season.

The directional distribution of the surface wind speeds shows that in summer easterly winds are somewhat stronger than westerly winds, while in winter, winds with a component from the northeast are stronger than winds with a component from the southwest. If the mean wind speed from each direction is considered representative of that sector, the mean summer and winter wind speeds are nearly the same at about 4 m.p.s.

The directional distribution of the mean shear components shows that the parallel component of the 1,000-m. wind is less than the surface speed for easterly wind directions, and exceeds the surface speed for westerly wind directions in both winter and summer. This would be expected from regional horizontal density gradients and from the station location with respect to the open sea. The normal component of the shear vector is directed to the left for all surface wind directions in all seasons, however, its magnitude is greatest for winds generally from the north, and least for southerly winds. The angular deviation of the 1,000-m. wind to the left of the surface wind, when averaged over all wind directions, is 24° in summer and 28° in winter.
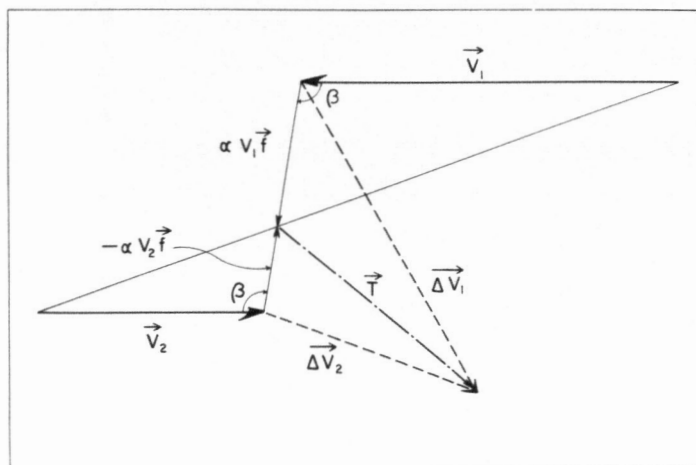

FIGURE 1.—Geometric constructions to determine the frictional and thermally produced shear vectors. $\mathbf{V}$ and $\Delta\mathbf{V}$ are the surface wind vectors and observed shear vectors, $\alpha\mathbf{V}_1\mathbf{t}$, and $\alpha\mathbf{V}_2\mathbf{f}$ are the frictionally produced wind shear vectors, and $\mathbf{T}$ is the thermal wind vector. See text for details of construction.

3. METHOD OF ANALYSIS

A single shear vector, which may represent the sum of the frictionally and thermally produced shear, may not uniquely be resolved into these two elements. It becomes necessary to take at least pairs of observed shear vectors and to make some assumptions about the structure of the wind profile within the boundary layer. Suitable assumptions are: that for each pair the thermal wind vector stays the same, that the angles formed by the frictional shear vectors and the surface wind are equal, and that the magnitude of the frictional shear vector is proportional to the surface wind speed. These assumptions correspond to a fixed geographic orientation of the thermal wind vector, and a fixed orientation of the frictional shear vector with respect to the surface wind direction; consequently, any angular difference between two surface wind vectors will be sufficient to determine uniquely the thermal and frictional shear vectors.

TABLE 1.—*Averaged surface wind, and component values of the observed wind shear between the surface and 1,000 m. by surface wind direction and season. Surface wind speed units are meters per second; shear units are meters per second per kilometer.*

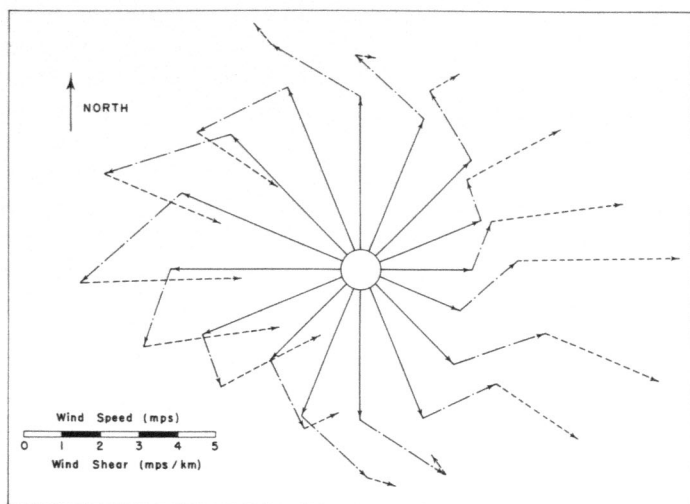|	Surface Wind Direction															
	N	NNE	NE	ENE	E	ESE	SE	SSE	S	SSW	SW	WSW	W	WNW	NW	NNW
SUMMER																
Surface wind	4.30	4.00	3.48	4.46	5.02	5.03	4.77	6.24	3.80	4.10	3.89	3.45	2.89	2.72	3.34	4.09
Shear component																
parallel	2.10	0.70	−0.51	−2.82	−2.80	−2.29	−1.30	−1.40	1.03	0.99	1.47	2.94	3.79	4.69	4.27	2.01
normal	−2.81	−2.96	−2.08	−1.12	−1.43	−1.37	−1.78	−1.29	−1.83	−1.65	−1.79	−1.39	−1.81	−3.37	−3.49	−3.56
WINTER																
Surface wind	6.19	6.09	3.98	3.17	3.91	3.84	4.00	2.78	3.10	3.36	3.30	3.23	2.58	2.73	3.13	5.52
Shear component																
parallel	0.70	0.34	−0.61	−0.66	−0.63	−0.11	0.76	0.54	0.80	2.71	3.01	4.11	4.31	2.93	1.87	0.72
normal	−3.48	−3.68	−2.56	−1.74	−1.73	−1.14	−1.04	−1.15	−2.38	−2.62	−2.56	−2.51	−2.50	−4.86	−6.06	−4.03

FIGURE 2.—Directional distribution of the surface wind vectors, frictionally produced shear vectors, and thermal wind vectors. Summer.
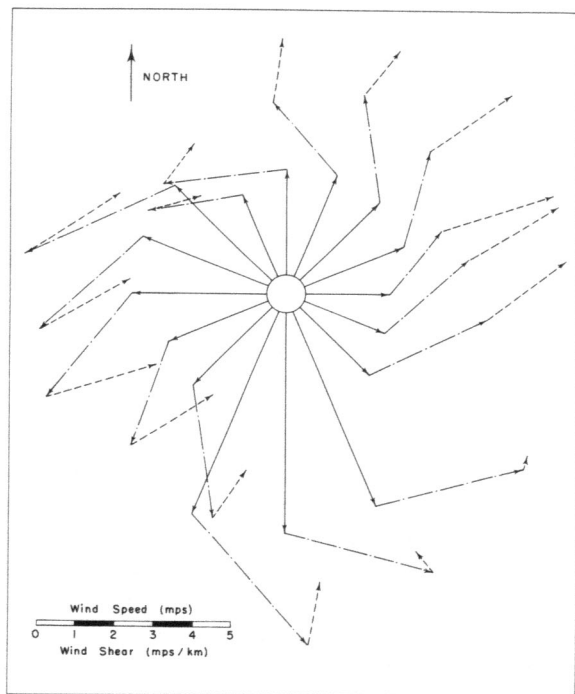

FIGURE 3.—Directional distribution of the surface wind vectors frictionally produced shear vectors, and thermal wind vectors. Winter.

The separation of the two shear vectors is most straight-forward if opposed wind directions are paired, as is shown in the example in figure 1. Vectors of surface wind and observed shear are drawn so that the heads of the observed shear vectors coincide. In this hypothetical Southern Hemisphere case, the east wind V_1, turns sharply to the left, while the west wind V_2, turns slowly to the right with altitude.

The following will explain the method in more detail. Since the thermal wind vector is assumed to be the same in both observations, and since the observed shear vectors were drawn to one point, we may allow the head of the thermal wind vector to fall on that point. It then follows that the heads of the frictional shear vectors for the two surface winds must also fall on one point, which must be the tail of the thermal wind vector. The second assumption, that the angles between the surface winds and the frictional shear vectors are the same, requires that this triple point lie on the line joining the heads of the two surface wind vectors. The third assumption, that the magnitude of each frictional shear vector is proportional to the corresponding surface wind, requires that this point coincide with the intersection of the lines joining the heads and the tails of the two surface wind vectors. In this example the frictional shear vector displaces the 1,000-m. wind vector 16° to the left of the surface wind vector, while the thermal wind vector displaces it toward the southeast. This has the effect of augmenting the rate of turning in the one case, and reversing it in the other.

Figures 2 and 3 show the observed shear vectors for the Little America data separated into frictional and thermal components in summer and winter. The frictional shear invariably has the effect of turning the wind vector to the left and increasing the speed with height. The amount of frictional turning of the wind vector from the surface to 1,000 m. varies from 17° to 28° in summer, and from 23° to 36° in winter. The seasonal difference may reflect greater hydrostatic stability in the boundary layer in winter, since the other effects on which the surface wind angle depends are either not applicable—variation with latitude—nor not very pronounced—variation with surface roughness (cf. Johnson [3]).

The angles themselves are somewhat greater than would be expected from theory. A representative geostrophic wind speed of 550 cm./sec., a Coriolis parameter of 1.42×10^{-4} sec.$^{-1}$, and surface roughness of 0.01 cm., which is typical of an Antarctic snow field, will produce an angle between the wind at the surface and at the top of the boundary layer of 15° (cf. H. Lettau [4]).

The effect of the thermal wind is to turn the surface wind vector toward an azimuth of 91° in summer, and toward an azimuth of 42° in winter. The effect is less pronounced for north or south winds than for east and west winds in both seasons, presumably because the effect of the temperature gradient at the edge of the ice near Little America is suppressed within a homogeneous air mass moving perpendicular to the shore. The largest thermal shears occur with zonal winds in summer, when the ice edge is much closer to the station and of nearly east-west orientation.

The change in direction of the thermal wind from summer to winter is related to the magnitude of the annual temperature variation in the area surrounding Little America. A shift such as that observed requires a much greater seasonal temperature contrast to the west and southwest than to the east and northeast of the station.
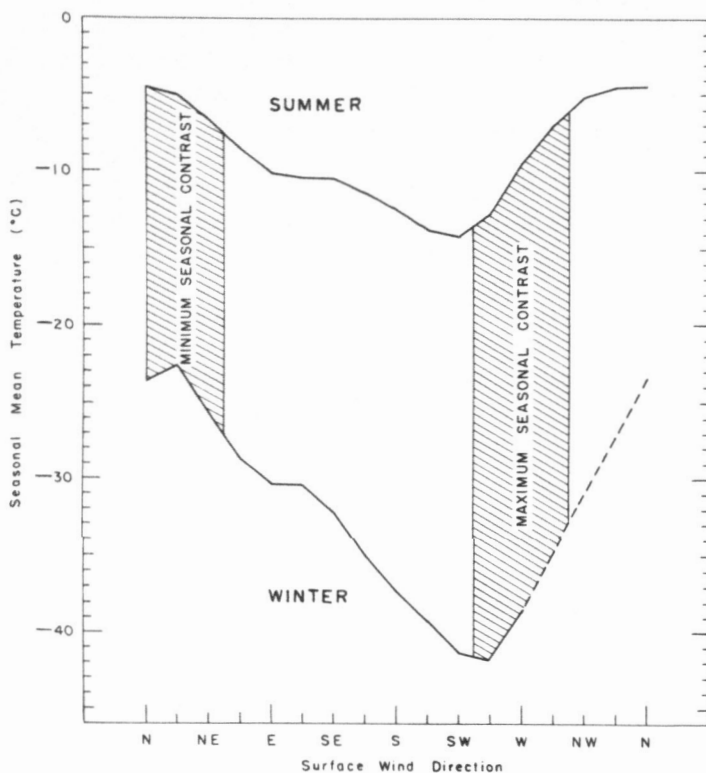
FIGURE 4.—Source region temperature as a function of the surface wind direction. The shaded areas show the directions of minimum and maximum seasonal temperature contrast.

Although the air temperatures in the vicinity of the station are not known directly, the seasonal contrast may be investigated by assuming that the mean temperature observed at the station with each wind direction is representative of thermal conditions some distance upwind. As shown in figure 4, the seasonal temperature contrast does vary with the wind direction, ranging from a minimum of about 18° C. for north-northeast winds to a maximum of about 28° C. for winds generally from the west. It is suggested therefore that both the orientation of the thermal wind vectors and the change from summer to winter are direct results of the local temperature distribution, rather than spurious geometrical values introduced by the method of analysis.

4. DETAILED WIND PROFILES

A more complete representation of the boundary layer may be obtained by a detailed analysis of the observed wind profiles. Since the thermal wind is apparently insensitive to changes in wind direction, this section has been limited to the examination of the mean profiles observed with north and south winds at the surface for both the summer and the winter seasons.

The theoretical background for the analysis of boundary layer wind profiles which include a constant thermal wind has been given by H. Lettau [5], H. Lettau and

Hoeber [6], and Johnson [3]. The assumptions are made that the large-scale motion is uniform and unaccelerated over level terrain of constant surface roughness, that there are no mean vertical motions, and that there are no inertial forces, and that the vertical density variation can be neglected. The wind velocity is then a function only of the pressure gradient and the vertical derivative of the shearing stress. If the coordinate system is oriented with the y-axis parallel and the x-axis normal to the direction of the surface stress, which is also the direction of the surface wind, the vertical variation of the geostrophic component parallel to the surface wind is constrained by the fact that the surface stress has no component normal to the y-direction, and that the shearing stress becomes negligible at height H. If $v(z)$ is the observed wind profile in the y-direction, and $V(z)$ the geostrophic wind profile in the same direction, then $\int_0^H (V-v)dz=0$. With the assumption of a constant thermal wind and geostrophic ambient conditions at $z=H=1,000$ m., $V(z)$ is represented by a straight line tangent to $v(z)$ at $z=1,000$ m., such that the algebraic sum of the differences $(V-v)$ (z) is zero. A similar line of reasoning will not give the analogous $U(z)$ since the surface stress parallel to the surface wind is not zero.

It is now possible to determine the vertical profile of τ_x,

$$\tau_x=\rho f\int_0^z (V-v)dz \qquad (1)$$

where ρ is the air density, and f is the Coriolis parameter. A similar expression can be written for τ_y,

$$\tau_y=\rho f\int_z^H (U-u)dz \qquad (2)$$

where $U(z)$ is the geostrophic wind profile and $u(z)$ the observed wind profile in the x-direction, although the relation is not very useful at the moment since neither the vertical profile of τ_y nor that of $U(z)$ is known. One may, however, also express the shearing stress at any level as the product of air density, wind shear, and eddy diffusivity. Both components of the wind shear are known and there is no reason to suppose the diffusivity to vary with direction. Thus for all values of z,

$$\frac{\tau_x}{\tau_y}=\frac{\partial u/\partial z}{\partial v/\partial z} \qquad (3)$$

in which τ_y is the only unknown. A convenient value to use is $z=z^*$, the height at which $V(z)$ and $v(z)$ intersect, which is the height of maximum τ_x. Thus $U(z)$ is obtained by the straight line tangent to $u(z)$ at $z=1,000$ m., such that

$$\tau_y(z^*)=\rho f\int_{z^*}^H (U-u)dz. \qquad (4)$$

Figures 5 through 8 show the above constructions for smoothed mean northerly and southerly wind profiles in
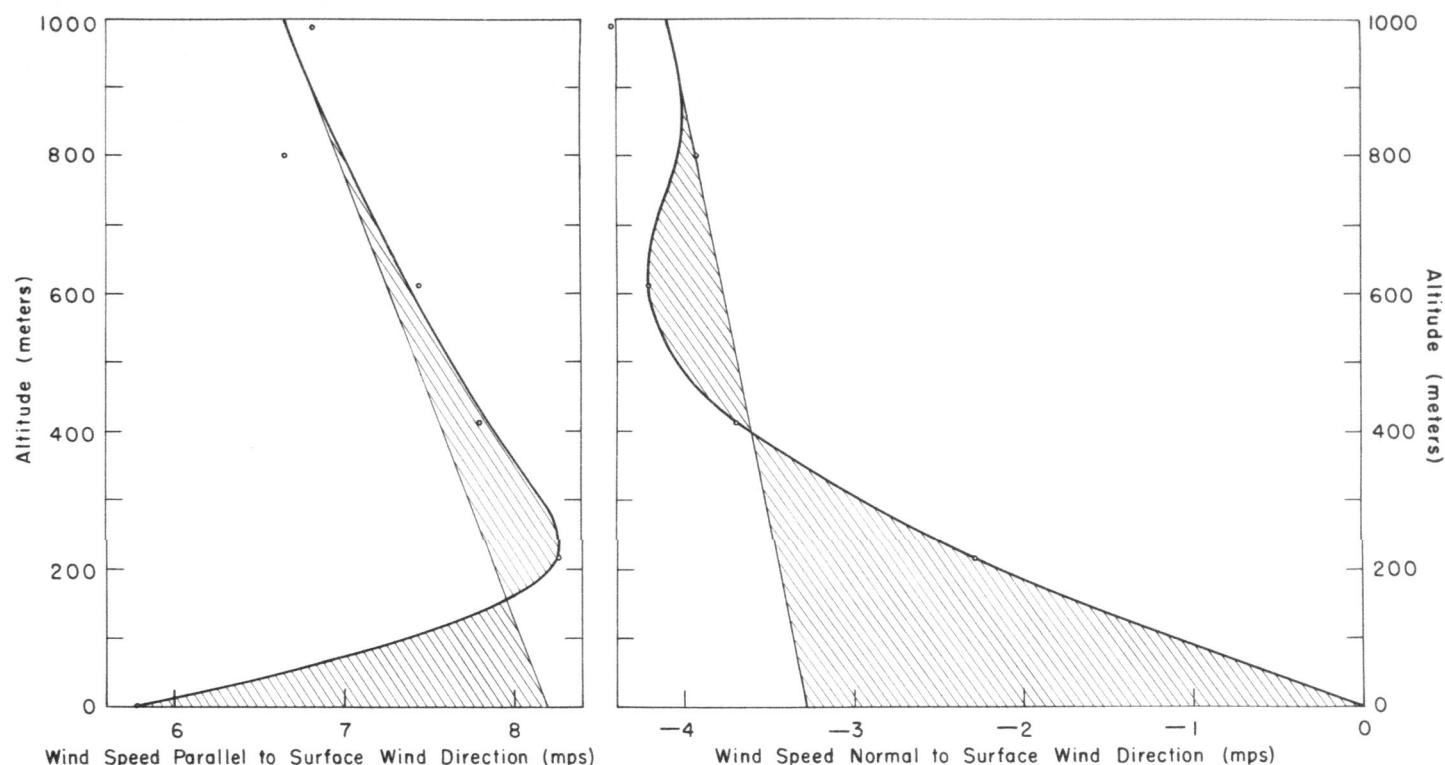
FIGURE 5.—Observed ambient mean wind profile and computed linear geostrophic wind profile separated into components parallel and normal to the surface wind direction. North winds in winter.

winter and summer. For the most part the differences among the four cases are minor, and related to directional rather than seasonal differences, suggesting that the ice surface produces its own characteristic wind distribution.

The component parallel to the surface wind increases with height immediately above the surface in all four cases, but reaches a maximum below 400 m. and decreases slowly with height above that level. The geostrophic wind decreases continuously in the boundary layer indicating that this component of the thermal wind is antiparallel to the surface wind. Its magnitude however is relatively small, ranging from 0.3 to 1.5 m. sec.$^{-1}$ km.$^{-1}$ The height at which τ_x reaches a maximum is approximately 160 m., with the exception of southerly winds in summer when

τ_x reaches a maximum at 200 m., and the maximum value attained ranges from 0.17 and 0.25 dyne/cm.^{2}

The component normal to the surface wind shows a definite directional difference, caused by the relatively fixed thermal wind vector. For the southerly winds this component increases from the surface to roughly 500 m., then decreases to the top of the boundary layer, the deviation being to the left of the surface wind. For the northerly winds the component value in summer increases continuously to the left of the surface wind through the boundary layer; in winter the profile is very similar with the exception of a slight relative maximum at 600 m. The geostrophic wind increases to the left for the northerly components, and to the right for the southerly components, implying an eastward-directed thermal wind for all cases.

TABLE 2.—*Derived boundary layer parameters at Little America*

| Parameter	Symbol	Units	North Winds		South Winds	
			Winter	Summer	Winter	Summer
Height of maximum τ_x	z^*	m.	155	160	162	202
Surface geostrophic wind	V_{g0}	m./sec.	8.78	5.81	6.23	6.15
Surface stress	τ_0	dyne/cm.^{2}	0.81	0.64	0.56	0.94
Surface geostrophic wind angle	α_0	degrees	22	24	23	34
Thermal wind vector						
magnitude	V_T	m. sec.$^{-1}$ km.$^{-1}$	1.72	1.24	1.47	1.42
azimuth		degrees	30	75	108	108
Surface Rossby number	Ro_g		8.32 x 10^6	2.76 x 10^6	4.57 x 10^6	0.045 x 10^6
Geostrophic drag coefficient	C		0.025	0.033	0.030	0.041
Energy dissipation	E	watts/m.^{2}	0.61	0.33	0.31	0.46
Roughness length	z_0	cm.	0.8	1.6	1.1	105
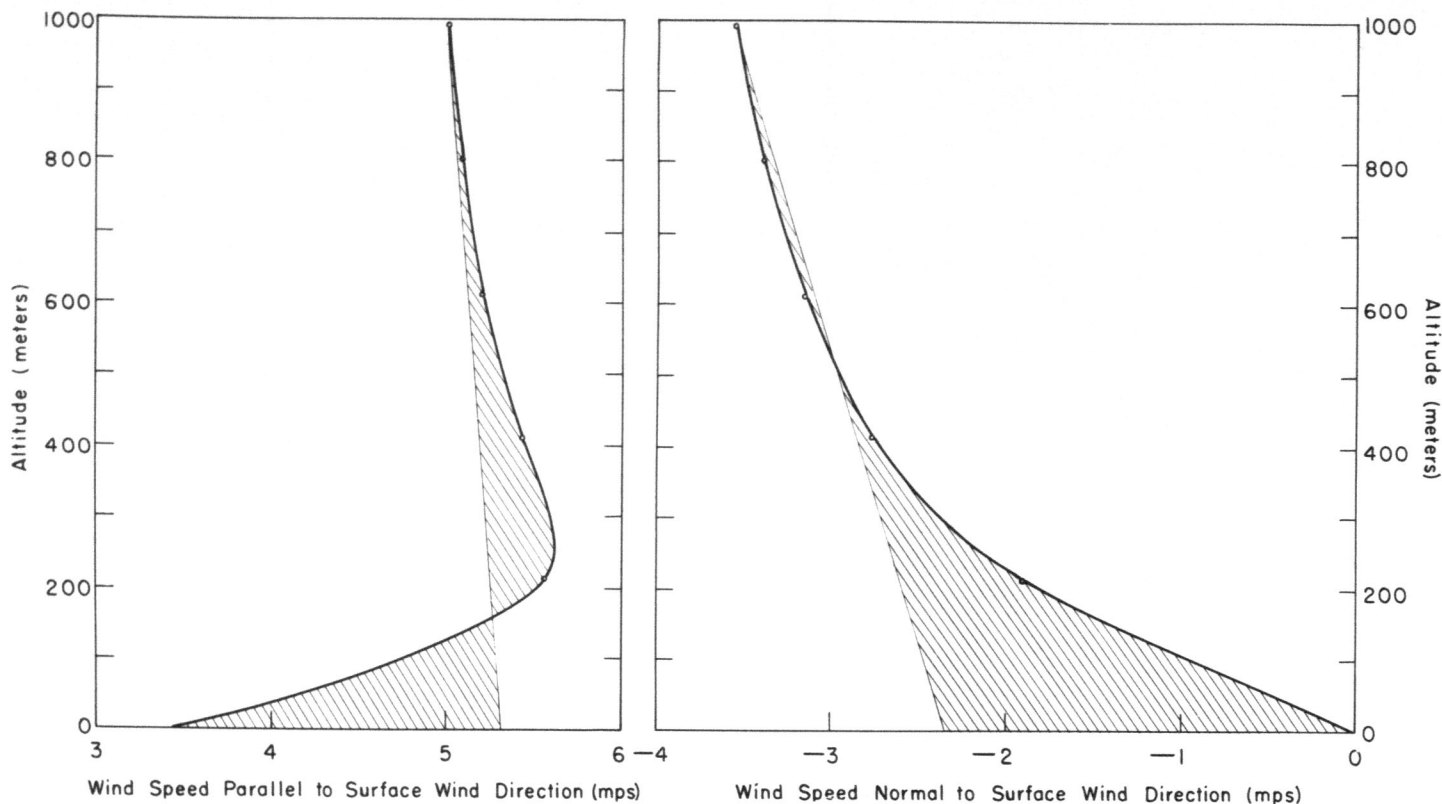
FIGURE 6.—Observed ambient mean wind profile and computed linear geostrophic wind profile separated into components parallel and normal to the surface wind direction. North winds in summer.

The magnitude of the normal component of the thermal wind is again relatively small, ranging from 0.8 to 1.4 m. sec.$^{-1}$ km.$^{-1}$

A number of other boundary layer parameters, given in table 2, may be determined either directly or sequentially from the observed and the geostrophic wind profiles. Those determined directly include the surface geostrophic wind, V_{g0}, obtained as the vector sum of the two geostrophic components at the surface, the surface stress, τ_0, determined from the relation

$$\tau_0 = \rho f \int_0^H (U-u)dz \qquad (5)$$

and the angle, α_0, between the surface geostrophic wind and the surface stress, determined by the arctangent of the ratio U_0/V_0. Derived parameters include the surface Rossby number, Ro_0, which is a unique function of the angle α_0, the geostrophic drag coefficient, C, determined by the relation

$$C = \sqrt{\frac{\tau_0}{\rho}} \frac{1}{V_{g0}}, \qquad (6)$$

the energy dissipated in jthe boundary layer, E, which may be obtained from the geostrophic wind and the surface stress (cf. H. Lettau [4]), and the roughness length, z_0, from the relation

$$z_0 = \frac{V_{g0}}{Ro_0 f}. \qquad (7)$$

The tabulated values are internally reasonably consistent with the exception of those parameter values derived from the surface geostrophic wind angle for the mean south wind profile in summer. The relatively much higher value for this angle produces a much lower surface Rossby number and consequently a much higher and quite spurious roughness length.

Similar analyses of wind profiles in the boundary layer have been undertaken by Johnson [3] for kite wind data from four stations in the midwestern United States, and by H. Lettau and Hoeber [6] for pilot balloon profiles obtained on Helgoland in the North Sea. Although all three studies are in reasonable agreement with one another, results of the first study are generally indicative of more vigorous flow over a rougher surface than that at Little America, while the second study shows more rapid air motion over a surface comparable to that at Little America. The differences in the surface stress and in the frictional energy dissipation within the boundary layer specifically emphasize these conclusions. At the inland stations in the first study the surface stress always exceeds 0.8 dyne/cm.^{2} and generally ranges from 1.5 to 2.0 dyne/cm.^{2}, while the energy dissipation generally exceeds 1
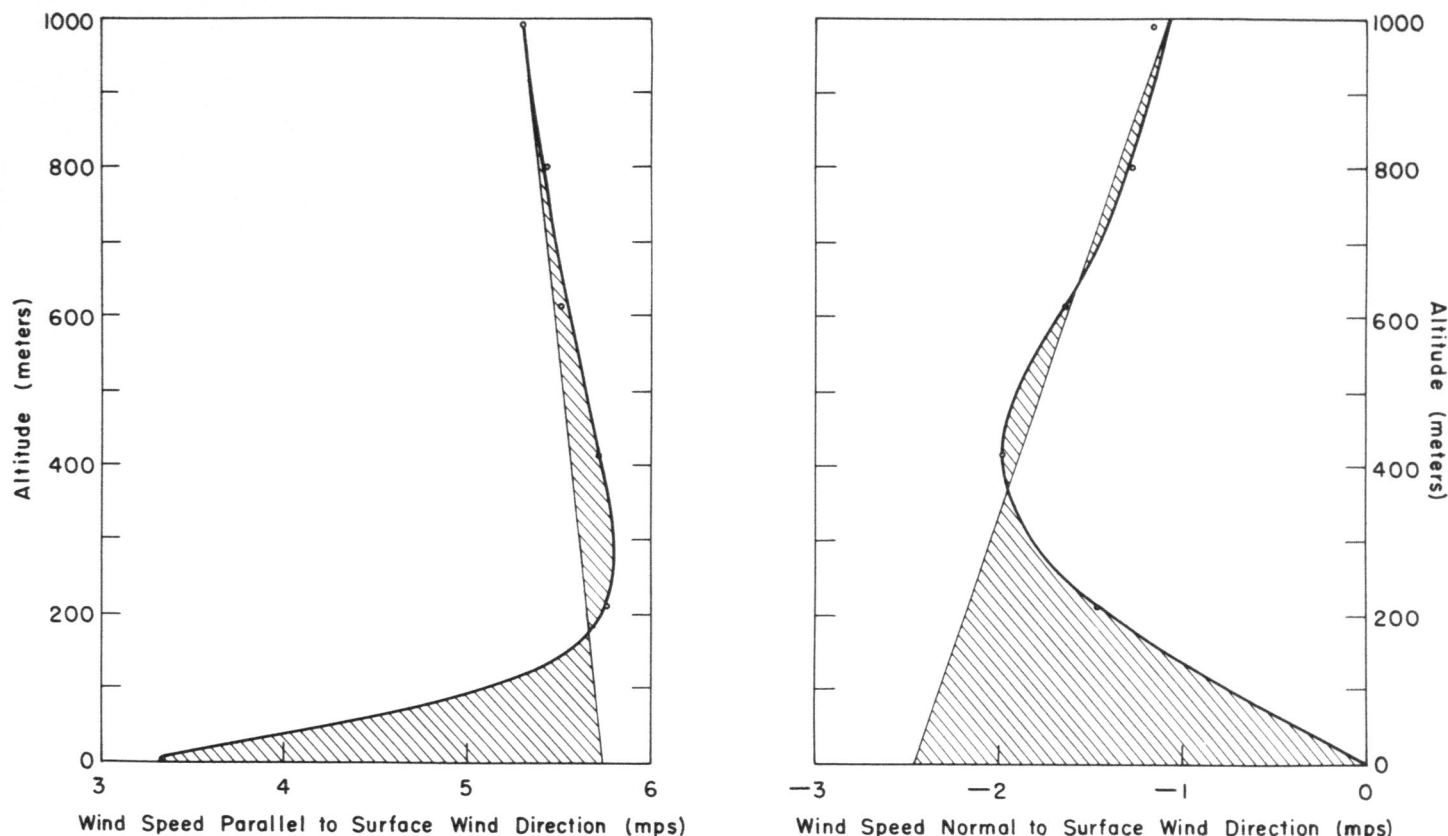
FIGURE 7.—Observed ambient mean wind profile and computed linear geostrophic wind profile separated into components parallel and normal to the surface wind direction. South winds in winter.

watt/m.^{2} On the ice shelf at Little America the stress ranges from about 0.6 to 0.9 dyne/cm.^{2}, and the energy dissipation from 0.3 to 0.6 watt/m.^{2}, lower by a factor of roughly three. The Helgoland data, which essentially represent wind profiles over a water surface, produce surface stress values of 0.6 and 0.9 dyne/cm.^{2}, and energy dissipation values of 0.6 and 1.4 watt/m.^{2} Since the surface stress value can be said to be determined by the shape of the wind profile components in the boundary layer, it is evident that these are roughly the same for the Helgoland and the Little America data. The energy dissipation values, on the other hand, also depend on the mean geostrophic wind in the boundary layer, which at Helgoland exceeds that at Little America by a factor of about two. Thus the observed difference is entirely due to the observed higher wind speed at Helgoland.

The computed angles between the surface geostrophic wind and the surface stress in the Little America data do not follow the similarity pattern described above. These are more nearly equal to those found for the inland data, which average about 25°, than to those found for the littoral data (9.5° and 11.2°). From this point of view the ice shelf is better described as a land surface than as a water surface.

A second point of similarity between the midwestern United States data and the Little America data is that the observed angles exceed by roughly 7° the values theoretically predicted by independently derived roughness lengths. If one takes the roughness length obtained as typical for the snow surface at the South Pole by Dalrymple et al. [1], $z_0 = 0.014$ cm., together with the observed wind speeds, one obtains a surface Rossby number of 3×10^8, which corresponds to an angle between the surface geostrophic wind and the surface stress of 17°. The difference, as obtained by Johnson [3], was attributed to a real height variation of the thermal wind which would become obscured by the method of analysis, rather than to topographical or other external effects. A similar real height variation of the thermal wind should be expected in the Little America data because of the complex thermal structure of the boundary layer which would produce a number of abrupt wind velocity changes rather than the smooth transition that has been shown here. The diabatic effects which should be considered on the ice shelf include radiational cooling near the ice surface, and temperature profiles which sometimes change from inversion to lapse conditions within the lowest 1,000 m.
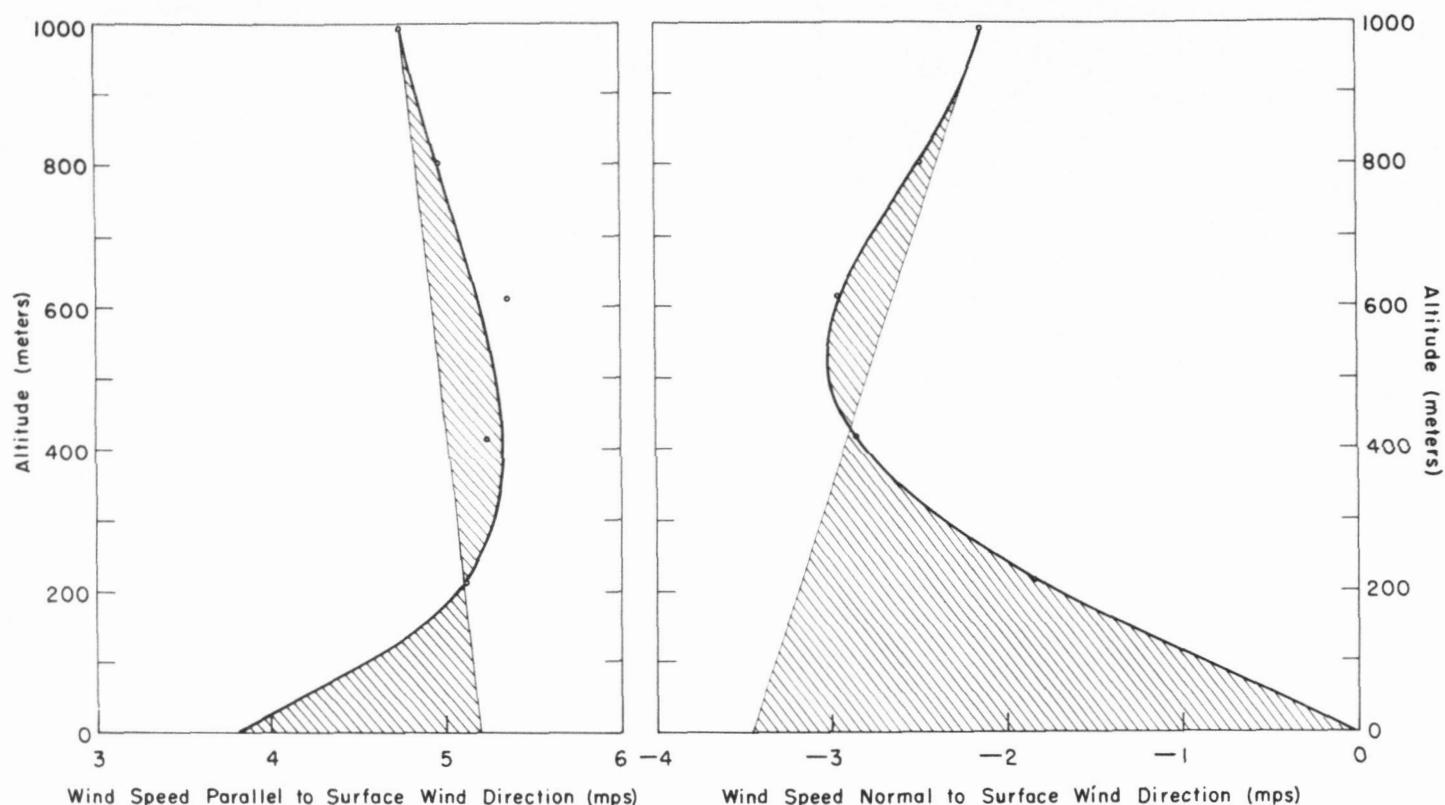
FIGURE 8.—Observed ambient mean wind profile and computed linear geostrophic wind profile separated into components parallel and normal to the surface wind direction. South winds in summer.

5. DISCUSSION

A hypothetical example of precisely such diabatic influences on the wind spiral near a snow surface has been prepared by H. Lettau [4]. Here a surface cooling rate of 26 langleys/day produced a significant reduction in the surface wind speed, and a correspondingly greater angle between the surface stress and the surface geostrophic wind vector than under adiabatic conditions. Although a surface inversion is in fact one of the major characteristics of the Antarctic boundary layer, it is not possible to investigate this diabatic effect in the Little America I and II data, since almost no free-air temperatures were obtained by the Byrd Antarctic Expeditions. Subsequent scientific efforts in the Antarctic have of course obtained simultaneous temperature and wind profiles, although none has matched the nearly 1,000 boundary layer profiles that have been used in this study to provide reliable mean values.

REFERENCES

1. P. C. Dalrymple, H. H. Lettau, and S. H. Wollaston, "South Pole Micrometeorology Program, Part II, Data Analysis," *Report* No. 20, Institute of Polar Studies, Ohio State University, 1963, 94 pp.
2. G. Grimminger and W. C. Haines, "Meteorological Results of the Byrd Antarctic Expeditions 1928–30, 1933–35: Tables," *Monthly Weather Review Supplement* No. 41, 1939, 377 pp.
3. W. B. Johnson, Jr., "Climatology of Atmospheric Boundary Layer Parameters and Energy Dissipation," *Studies of the Three-Dimensional Structure of the Planetary Boundary Layer*, Dept. of Meteorology, University of Wisconsin, 1962, pp. 125–158.
4. H. H. Lettau, "Notes on Theoretical Models of Profile Structure in the Diabatic Surface Layer," *Studies of the Three-Dimensional Structure of the Planetary Boundary Layer*, Dept. of Meteorology, University of Wisconsin, 1962, pp. 195–226.
5. H. H. Lettau, "Windprofil, innere Reibung, und Energie Umsatz in den unteren 500 m. über dem Meer," *Beiträge zur Physik der Atmosphäre*, vol. 30, No. 2, 1957, pp. 78–96.
6. H. H. Lettau and H. Hoeber, "Über die Bestimmung der Höhenverteilung von Schubspannung und Austauschkoeffi-zienten in der atmosphärischen Reibungsschicht," *Beiträge zur Physik der Atmosphäre*, vol. 37, No. 2, 1964, pp. 105–118.